The most elementary Bell inequalities

Muhamad Sadiq,[1] Piotr Badziąg,[1] Mohamed Bourennane,[1] and Adán Cabello[2, 1]

[1]*Department of Physics, Stockholm University, S-10691, Stockholm, Sweden*
[2]*Departamento de Física Aplicada II, Universidad de Sevilla, E-41012 Sevilla, Spain*
(Dated: June 24, 2011)

Every nontrivial Bell inequality can be associated to a graph with some special properties. The simplest of these graphs is the pentagon. In this sense, any Bell inequality associated to a pentagon can be regarded as elementary. We show that there are three of them: one is a primitive Bell inequality inside the Clauser-Horne-Shimony-Holt inequality and, surprisingly, it is not maximally violated by maximally entangled states. The other two are maximally violated by maximally entangled states and are related to the Clauser-Horne inequality and the I_{3322} inequality, respectively. We report experimental violations of the three inequalities with pairs of photons entangled in polarization.

Introduction.—Contrary to classical intuition, nature allows for violations of noncontextuality and local realism. The degree and conditions for these violations are today routinely tested in experimental probing of noncontextual and Bell inequalities. The inequalities are linear combinations of probabilities of propositions of the type "the results $a, b, \ldots, c$ are respectively obtained when the measurement $x, y, \ldots, z$ are performed," denoted by $ab \ldots c | xy \ldots z$. In noncontextual inequalities, $x, y, \ldots, z$ are mutually compatible measurements [1]; additionally, in Bell inequalities the measurements $x, y, \ldots, z$ should be spacelike separated. Therefore, any Bell inequality is a noncontextual inequality with extra requirements, but noncontextual inequalities are more general and include inequalities violated by sequential measurements on noncomposite systems [2–5].

It has been recently found that there is a one-to-one correspondence between noncontextual inequalities and graphs [6]: the classical, quantum, and general probabilistic bounds of the inequalities are given by three characteristic numbers of the graph which can be efficiently calculated. With regard to Bell inequalities, the graph approach provides the maximum quantum violation in most cases; but there are examples, like the I_{3322} Bell inequality [7–9], in which it only provides an upper bound.

The aim of this contribution is to single out, classify, and experimentally test all the simplest and most elementary Bell inequalities from the graph perspective; that is the Bell inequalities represented by the simplest graphs. In addition, our analysis will explain why, in general, the graph approach only provides an upper bound to the maximum quantum violation of a Bell inequality, and establishes the basis for solving this problem.

Every experiment can be regarded as a set of tests for the frequencies (probabilities) with which propositions $ab \ldots c | xy \ldots z$ are true. Each of these propositions can be represented by a vertex of a graph G such that edges link mutually exclusive propositions. The sum of the probabilities tested in the experiment is bounded differently depending on the underlying physical theory used to analyze the experiment. In [6], it is shown that the classical bound is given by the graph's independence number $\alpha(G)$ [10], the quantum bound by the Lovász number $\vartheta(G)$ [11], and the bound for general probabilistic theories by the fractional packing number $\alpha^*(G)$ [12].

The pentagon is the simplest graph with $\vartheta(G) > \alpha(G)$ (c.f. Supplementary Information, Sec. A). The fact that the classical, quantum, and general probabilistic bounds of the sum of five pairwise exclusive propositions are different was first pointed out in [13]. The pentagon is behind noncontextual inequalities [2, 14] recently tested in experiments [15, 16]. The question is whether there are Bell inequalities with this structure.

In a bipartite Bell scenario, the propositions are reduced to "Alice measures x and obtains a, and Bob measures y and obtains b." Such propositions are denoted by $ab|xy$. The probability that $ab|xy$ is true is then $P(ab|xy)$. The edges of a bipartite graph G link these (and only these) pairs of vertices $ab|xy$ and $a'b'|x'y'$ for which $x = x'$ and $a \neq a'$ or $y = y'$ and $b \neq b'$.

Within this paradigm, every bipartite Bell inequality with rational coefficients can be put into the following form:

$$\sum_{ab|xy \in G} P(ab|xy) \leq \Omega. \tag{1}$$

This is because every probability with a negative coefficient in the standard formulation can be substituted by one minus the probability of the complementary proposition. The upper bound Ω depends on the underlying physical theory. We will consider local theories (Ω_{L}), quantum mechanics (Ω_{QM}), and general probabilistic theories Ω_{GP}.

We examined all possible assignments of the propositions $ab|xy$ to the pentagon, and found that there are three nonequivalent Bell inequalities associated to it.

First Bell inequality.—One set of local propositions satisfying the constraints of the pentagon is shown in
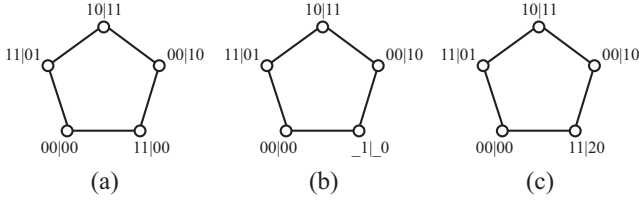
FIG. 1. Assignments of propositions corresponding to the first (a), second (c), and third (c) Bell inequality.

Fig. 1 (a). The corresponding Bell inequality,

$$P(00|00)+P(11|01)+P(10|11)+P(00|10)+P(11|00) \le 2, \tag{2}$$

is a two-setting two-outcome (both for Alice and Bob) Bell inequality. The local bound is $\Omega_{\mathrm{L}} = \alpha(C_5) = 2$ (C_5 denotes a pentagon). The maximum quantum value is upper bounded by $\theta(C_5) = \sqrt{5} \approx 2.236$. Nevertheless, the maximum *bipartite* quantum violation for the inequality (c.f. Supplementary Information, Sec. B) is only $\Omega_{\mathrm{QM}} \approx 2.171$. It occurs for states and settings locally equivalent to

$$|\psi\rangle = 0.7974|00\rangle + 0.60345|11\rangle, \tag{3}$$

and

$$P(00|00) = |(c, -s) \otimes (-s, c)|\psi\rangle|^2, \tag{4a}$$
$$P(11|01) = |(s, c) \otimes (-C, -S)|\psi\rangle|^2, \tag{4b}$$
$$P(10|11) = |(S, C) \otimes (-S, C)|\psi\rangle|^2, \tag{4c}$$
$$P(00|10) = |(C, -S) \otimes (-s, c)|\psi\rangle|^2, \tag{4d}$$
$$P(11|00) = |(s, c) \otimes (c, s)|\psi\rangle|^2, \tag{4e}$$

respectively, with $c = 0.5812$, $s = 0.8137$, $C = 0.9864$, and $S = 0.1644$. Interestingly, the inequality is maximally violated by nonmaximally entangled sates.

This is interesting since (as we will see later) inequality (2) can be regarded as a primitive building block in the Clauser-Horne-Shimony-Holt (CHSH) inequality [17], which is maximally violated by maximally entangled states only.

Second Bell inequality.—Relaxation of the symmetry between Alice's and Bob's actions in (2) allows one to substitute Alice's measurement in vertex 11|00 of Fig. 1 (a) with the identity (deterministic *yes*). The substitution produces a set of propositions depicted in Fig. 1 (b) and a new Bell inequality,

$$P(00|00)+P(11|01)+P(10|11)+P(00|10)+P(\_1|\_0) \le 2, \tag{5}$$

where $P(\_1|\_0)$ denotes the probability of Bob obtaining 1 when measuring in setting 0 irrespectively of Alice's action. Nonsignalling requires that, for all settings x, x', and y, and for all results b, $P(\_b|xy) = P(\_b|x'y) = P(\_b|\_y)$.

The maximum bipartite quantum value for the left-hand side of (5) is $\Omega_{\mathrm{QM}} = \frac{3+\sqrt{2}}{2} \approx 2.207$, which is larger than the one for inequality (2) but still strictly below $\sqrt{5}$. The bipartite bound is achieved with maximally entangled states, e.g. with $|\phi^+\rangle = \frac{1}{\sqrt{2}}(|00\rangle + |11\rangle)$, with the settings

$$P(00|00) = |(0, 1) \otimes (-s, c)|\phi^+\rangle|^2, \tag{6a}$$
$$P(11|01) = |(1, 0) \otimes (-c, s)|\phi^+\rangle|^2, \tag{6b}$$
$$P(10|11) = |(1/\sqrt{2}, 1/\sqrt{2}) \otimes (s, c)|\phi^+\rangle|^2, \tag{6c}$$
$$P(00|10) = |(-1/\sqrt{2}, 1/\sqrt{2}) \otimes (-s, c)|\phi^+\rangle|^2, \tag{6d}$$

with $c = \cos\left(\frac{\pi}{8}\right)$ and $s = \sin\left(\frac{\pi}{8}\right)$. In an ideal experiment, the first four probabilities are $\frac{c^2}{2} \approx 0.427$, while $P(\_1|\_0) = \frac{1}{2}$.

Third Bell inequality.—Without changing the bipartite quantum bound, one can substitute the optimal one-dimensional projection for the identity measurement of Alice in Fig. 1 (b). This leads to a vertex allocation depicted in Fig. 1 (c) and a genuine three-setting (in Alice's side) two-setting (in Bob's) two-outcome Bell inequality

$$P(00|00)+P(11|01)+P(10|11)+P(00|10)+P(11|20) \le 2. \tag{7}$$

Now the optimal local settings are the same as those of inequality (5), with Alice's additional measurement projecting on (c, s) and producing $P(11|20) = |(c, s) \otimes (c, s)|\phi^+\rangle|^2$.

The three inequalities (2), (5), and (7) exhaust the list of the Bell inequalities extractable from a pentagon. All three are maximally violated by pairs of qubits and nothing can be gained by using larger physical systems (cf. Supplementary Information, Sec. B).

Connection to previous Bell inequalities.—The most well known form of the CHSH inequality is

$$-2 \le \langle A_0 B_0 \rangle + \langle A_0 B_1 \rangle + \langle A_1 B_0 \rangle - \langle A_1 B_1 \rangle \le 2, \tag{8}$$

where $\langle A_i B_j \rangle$ denotes the average of the product of the outcomes (± 1) of the results of Alice's measurement A_i and Bob's measurement B_j.

With the help of $\langle A_i A_j \rangle = P(00|ij) + P(11|ij) - P(01|ij) - P(10|ij)$ and $-\langle A_i A_j \rangle = 2P(01|ij) + 2P(10|ij) - 1$, the inequality can be easily rewritten as

$$P(00|00) + P(11|00) + P(00|01) + P(11|01) + \\ P(00|10) + P(11|10) + P(01|11) + P(10|11) \le 3. \tag{9}$$

The sum corresponds to a $(1, 4)$-circulant graph on 8 vertices, $Ci_8(1, 4)$ (see Fig. 2). For this graph, $\alpha[Ci_8(1, 4)] = 3 = \Omega_{\mathrm{L}}$, $\vartheta[Ci_8(1, 4)] = 2 + \sqrt{2} \approx 3.414 = \Omega_{\mathrm{QM}}$, and $\alpha^*[Ci_8(1, 4)] = 4 = \Omega_{\mathrm{GP}}$. The bounds derived from the graph's structure equal the local realistic, quantum (Tsirelson), and the general probabilistic (nonsignalling) bound respectively. It is also easy to notice that the graph in Fig. 2 consists of 8 overlapping pentagons like
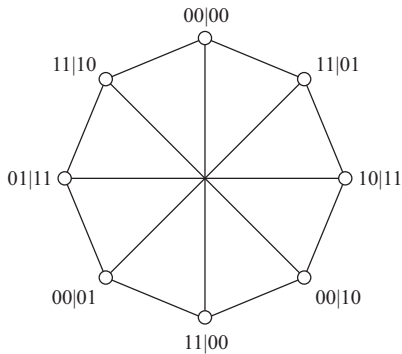
FIG. 2. Graph corresponding to the CHSH inequality (9).

FIG. 3. Experimental setup for testing the Bell inequalities.

the one in Fig. 1 (a). In other words, the CHSH inequality can be regarded as consisting of 8 pentagonal Bell inequalities. The non classical properties of $Ci_8(1,4)$ can thus be traced back to those of the pentagon. In this sense, inequality (2) represents a primitive basic block inside the CHSH inequality.

Inequality (9) is not the only form of the CHSH inequality in terms of the sum of probabilities. With the help of identities like $P(11|xy) = 1 - P(0\_|x\_) - P(10|xy)$ and $P(10|xy) = P(\_0|\_y) - P(00|xy)$, it can be transformed into the Clauser-Horne (CH) inequality [18], whose terms can be rearranged into inequality (5). The interesting fact here is that while $\vartheta(Ci_8(1,4))$ provides the exact maximum quantum violation, $\vartheta(C_5)$ only provides an upper bound.

Regarding inequality (7), the I_{3322} inequality can be rewritten in a form related to a 10-vertex graph containing the pentagon of (7) as a subgraph (see Supplementary Information, Sec. C).

Experimental violations.—We have tested the maximum quantum violation of the three Bell inequalities using pairs of photons entangled in polarization. In the experiment, UV light-pulses centered at wavelength of 390 nm (pulse length 130 fs, repetition rate 82 MHz) were focused inside a 2 mm thick BBO (β barium borate) nonlinear crystal, to produce photon pairs emitted into two spatial modes a and b through the second order degenerate emission of type-II spontaneous parametric down-conversion. The emitted photons were coupled into single mode optical fibers (length 2 m) and passed through a narrow-bandwidth interference filters (F) ($\Delta\lambda = 1$ nm) to secure well defined spatial and spectral emission modes. To observe $|\phi_+\rangle$ and $|\psi\rangle$, a half waveplate (HWP) was placed after the output fiber coupler in mode (b). The polarization measurement was performed using HWPs and polarizing beam splitters (PBS) followed by actively quenched Si-avalanche photodiodes (Si-APD) (see Fig. 3). The measurement time for each setting was 100 seconds. The results of the tests of the Bell inequalities (2), (5), and (7) are presented in Tables I, II, and III, respectively.
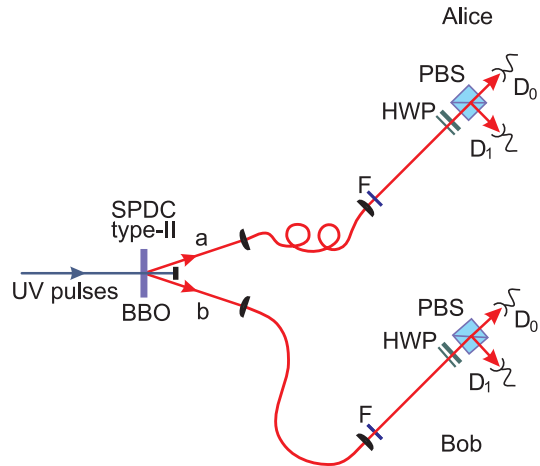
One may notice that, in the experiment, the left-hand side (LHS) of inequality (5) comes noticeably closer to Ω_{QM} than the LHC of (7), despite both have the same bipartite quantum bound Ω_{QM}. This is not unexpected, since measuring (7) requires more measurements on Alice's side which in turn expands the scope for errors.

Bell inequalities versus general noncontextual inequalities.—The previous discussion illustrates in the simplest possible way the difference between Bell inequalities and noncontextual inequalities. Bell inequalities can be regarded as noncontextual inequalities having extra restrictions. The first is that the propositions allowed in a Bell inequality experiment concern only local measurements. The second is that, for a bipartite Bell experiment, exclusiveness between two propositions can happen for three different reasons: (i) exclusiveness between Alice's propositions (e.g., between 00|00 and 11|01), (ii) exclusiveness between Bob's propositions (e.g., between 00|00 and 11|10), and (iii) both (i) and (ii) (e.g., between 00|00 and 11|00). The graph does not give information about these extra restrictions. The fact that this information is relevant is illustrated by the three (inequivalent) inequalities corresponding to a pentagon. This suggests that, to obtain the maximum violation of a Bell inequality, two graphs, one for Alice's propositions and one for

TABLE I. Experimental results for the test of inequality (2).

	Experimental	Optimal
$P(00|00)$	0.404 ± 0.012	0.439
$P(11|01)$	0.476 ± 0.012	0.487
$P(10|11)$	0.314 ± 0.011	0.320
$P(00|10)$	0.413 ± 0.013	0.487
$P(11|00)$	0.481 ± 0.012	0.439
Ω_{QM}	2.088 ± 0.027	2.171

Bob's, are needed. An open question is whether this approach admits a solution as a semidefinite program (as it happens with the calculation of the graph's Lovász number) or requires something as complex as solving the hierarchy of semidefinite programs proposed in [19].

Conclusion.—In summary, we have shown how graphs generate nontrivial Bell inequalities. The graph gives information about the local, quantum, and general probabilistic bounds of the Bell inequality. Using this approach, we have identified and tested the three nonequivalent elementary bipartite Bell inequalities based on the simplest graph with a quantum-classical gap, the pentagon. One of the inequalities can be identified as the building block of the CHSH inequality, the second as a part in one version of this inequality, and the third as a part of a simple form of the I_{3322} inequality.

Our approach suggests a possibility of Bell inequalities *à la carte*, where one would start by singling out a graph with promising properties (for example, a quantum-classical gap with the highest robustness against noise for a given number of experimental contexts), and then explore whether this graph would admit an assignment of propositions corresponding to a Bell inequality. In addition, it suggests a new method to calculate the (exact) maximum quantum violation of any Bell inequality from the properties of graphs containing the exclusiveness relations among Alice and Bob's propositions separately. This problem will be addressed in a future work.

Finally, one may notice that while previous tests of pentagonal inequalities using sequential measurements [15, 16] suffer the compatibility loophole [5], our experiments are free of this loophole, since the perfect compatibility is guaranteed by the space separation between the measurements.

[1] A. Peres, *Quantum Theory: Concepts and Methods* (Kluwer, Dordrecht, 1995), p. 203.
[2] A. A. Klyachko, M. A. Can, S. Binicioğlu, and A. S. Shumovsky, Phys. Rev. Lett. **101**, 020403 (2008).
[3] A. Cabello, Phys. Rev. Lett. **101**, 210401 (2008).
[4] P. Badziąg, I. Bengtsson, A. Cabello, and I. Pitowsky, Phys. Rev. Lett. **103**, 050401 (2009).
[5] O. Gühne *et al.*, Phys. Rev. A **81**, 022121 (2010).
[6] A. Cabello, S. Severini, and A. Winter, arXiv:1010.2163.
[7] M. Froissart, Nuov. Cim. B **64**, 241 (1981).
[8] C. Śliwa, Phys. Lett. A **317**, 165 (2003).
[9] D. Collins and N. Gisin, J. Phys. A: Math. Gen. **37**, 1775 (2004).
[10] R. Diestel, *Graph Theory*, Graduate Texts in Mathematics **173** (Springer, Heidelberg, 2010).
[11] L. Lovász, IEEE Trans. Inf. Theory **25**, 1 (1979).
[12] E. R. Scheinerman and D. H. Ullman, *Fractional Graph Theory*, Wiley-Interscience Series in Discrete Mathematics and Optimization (John Wiley & Sons, New York, 1997).
[13] R. Wright, in *Mathematical Foundations of Quantum Mechanics*, edited by A. R. Marlow (Academic Press, San Diego, 1978), p. 255.
[14] P. Badziąg, I. Bengtsson, A. Cabello, H. Granström, and J.-Å. Larsson, Found. Phys. **41**, 414 (2011).
[15] R. Łapkiewicz *et al.*, Nature (London) **474**, 490 (2011).
[16] J. Ahrens, E. Amselem, M. Bourennane, and A. Cabello (unpublished).
[17] J. F. Clauser, M. A. Horne, A. Shimony, and R. A. Holt, Phys. Rev. Lett. **23**, 880 (1969).
[18] J. F. Clauser and M. A. Horne, Phys. Rev. D **10**, 526 (1974).
[19] M. Navascués, S. Pironio, and A. Acín, New J. Phys. **10**, 073013 (2008).

TABLE II. Experimental results for the test of inequality (5).

	Experimental	Optimal
$P(00\|00)$	0.378 ± 0.012	0.427
$P(11\|01)$	0.466 ± 0.013	0.427
$P(10\|11)$	0.384 ± 0.012	0.427
$P(00\|10)$	0.381 ± 0.013	0.427
$P(\_1\|\_0)$	0.544 ± 0.013	0.5
$\Omega_{\rm QM}$	2.154 ± 0.028	2.207

TABLE III. Experimental results for the test of inequality (7).

	Experimental	Optimal
$P(00\|00)$	0.378 ± 0.012	0.427
$P(11\|01)$	0.466 ± 0.013	0.427
$P(10\|11)$	0.384 ± 0.012	0.427
$P(00\|10)$	0.381 ± 0.013	0.427
$P(11\|20)$	0.529 ± 0.013	0.5
$\Omega_{\rm QM}$	2.139 ± 0.028	2.207

SUPPLEMENTARY INFORMATION

A. The pentagon is the simplest graph with a quantum-classical gap

A graph G corresponds to an experiment in which quantum correlations are larger than quantum correlations if and only if $\alpha(G) < \theta(G)$. As seen in Fig. 4, the pentagon is the simplest graph, and the only one with up to 5 vertices, with this property.

B. Bell inequalities associated to the pentagon

Two qubits are enough.—Consider a positive Bell operator $\tilde{\mathcal{B}}$ and let the operator's support span an n-dimensional space $H_n \subset H$. Every normalized vector $|a\rangle \in H$ can be decomposed into the following combination of two normalized vectors $|a_{in}\rangle \in H_B$ and $|a_\perp\rangle \in B - H_n$: $|a\rangle = \sin(\theta)|a_{in}\rangle + \cos(\theta)|a_\perp\rangle$. Consider now an operator $\mathcal{B} = \tilde{\mathcal{B}} + |a\rangle\langle a|$.

Observation: With a given $|a_{in}\rangle$, the largest eigenvalue of $\mathcal{B}$ achieves its maximum with respect to θ for $\sin(\theta) = 1$.

Proof: The expectation value of $\mathcal{B}$ on an arbitrary normalized vector $|v\rangle = |v_{in}\rangle + |v_\perp\rangle$ can be written in the following form:

$$\langle v|B|v\rangle = \langle v_{in}|\tilde{\mathcal{B}}|v_{in}\rangle + |\sin(\theta)\langle a_{in}|v_{in}\rangle + \cos(\theta)\langle a_\perp|v_\perp\rangle|^2. \tag{10}$$

This expression is to be maximized with respect to angle θ and a normalized vector $|v\rangle = |v_{in}\rangle + |v_\perp\rangle$. Without influencing the first term in the sum in (10), one can make the phase of $\langle a_\perp|v_\perp\rangle$ the same as the phase of $\langle a_{in}|v_{in}\rangle$. The second term can be then maximized with respect to θ by taking $\theta = \arctan\left(\frac{\langle a_{in}|v_{in}\rangle}{\langle a_\perp|v_\perp\rangle}\right)$. This converts (10) into

$$\langle v|B|v\rangle = \langle v_{in}|\tilde{\mathcal{B}}|v_{in}\rangle + |\langle a_{in}|v_{in}\rangle|^2 + |\langle a_\perp|v_\perp\rangle|^2. \tag{11}$$

Due to normalization of $|v\rangle$, one can write $|v_{in}\rangle = \cos(\phi)|u_{in}\rangle$ and $|v_\perp\rangle = \sin(\phi)|u_\perp\rangle$, with $|u_{in}\rangle$ and $|u_\perp\rangle$ normalized. This brings the sought for expectation value to

$$\langle v|B|v\rangle = \cos^2(\phi)\langle u_{in}|\tilde{\mathcal{B}} + |a_{in}\rangle\langle a_{in}|u_{in}\rangle + \sin^2(\phi)|\langle a_\perp|u_\perp\rangle|^2. \tag{12}$$

Since, for any normalized $|a_{in}\rangle \in H_n$, the maximum eigenvalue of $\tilde{\mathcal{B}} + |a_{in}\rangle\langle a_{in}|$ is not less than one, the maximum of the right hand side of (12) occurs for $\cos^2(\phi) = 1$, which implies $\langle a_\perp|v_\perp\rangle = 0$ and, consequently $\sin(\theta) = 1$. ∎

The observation indicates that an optimal Bell operator is likely to be confined to the Hilbert space of minimum dimension allowed by the orthogonality relations in the graph. For the pentagon this is actually conclusive.

To produce a nontrivial Bell inequality, the settings associated to the vertices of the pentagon must span $\mathcal{C}^2 \times \mathcal{C}^2$. According to the observation, the optimal fifth vector should lie (if possible) in this space.

Optimization.—In a bipartite scenario, the orthogonality represented by a graph's edge can be two-fold: orthogonality between Alice's projectors (type A edge) or orthogonality between Bob's projectors (type B edge). The possible case when both pairs are orthogonal can then be regarded as either A or B. With this classification there are four essentially different edge patterns in a pentagon: those containing four AB vertexes (edge pattern $ABABA$), those containing two AB vertexes (edge patterns $AAABB$ and $AAAAB$), and those where orthogonality is confined to one party (edge pattern $AAAAA$). This last case is essentially local. There, Bob acts only as a dummy. Thus any possible violation of the underlying inequality is due to contextuality local to Alice and not to any nonclassical correlations between the measurement results of Alice and Bob. Therefore we excluded this case from our considerations. A possible way of formalizing such an exclusion is to restrict the dimensionality of the local spaces addressed in the experiments to less than what is required by the structure of the graph. A pentagon requires, e.g. $\mathcal{C}^3$ to implement its orthogonality pattern. To exclude the trivial case one can then demand that neither party has a bigger local system than one qubit.

Numerical optimization of the remaining cases strongly indicate that only case (four AB vertexes) produces a violation of the inequality. For that case we could even identify the analytical expressions for the vectors on which the corresponding questions project.

Real vectors are enough.—The numerical search for optimal projectors could be confined to real vectors. To see that this is so, one can number the vertexes as $0, \ldots, 4$, assume a given orthogonality pattern (here $ABABB$) and denote the (product) vector on vertex 0 as $|v_0\rangle = |00\rangle$. The (so far arbitrary) vector on vertex 2 can be denoted by $|v_2\rangle = |P(\perp)u\rangle$ (symbols $|x\rangle$ and $|x_\perp\rangle$ denote mutually orthogonal vectors). Both $|P(\perp)\rangle$ and $|u\rangle$ can be made real by adjusting the phase of the local basis vectors $|1_A\rangle$ and $|1_B\rangle$. This will make vectors $|p\rangle$ and $|u_\perp\rangle$ real too. The vector at vertex 1 is now determined by the assumed orthogonality pattern. It has to be real and equal to $|1u_\perp\rangle$. The pattern and the already determined vectors specify $|v_4\rangle = |x1\rangle$ and $|v_3\rangle = |py\rangle$. Finally, orthogonality of vertexes 3 and 4 together with the assumed pattern requires that $|y\rangle$ is orthogonal to $|1_B\rangle$, which will optimize (c.f. Confine Hilbert space) to $|y\rangle = |0_B\rangle$. Alice's vector $|x\rangle$ remains arbitrary in this construction. Moreover, the pentagon does not contain its orthogonal partner. Thus in order to optimize the Bell operator, one can replace the projection on $|x\rangle$ by the identity operator.
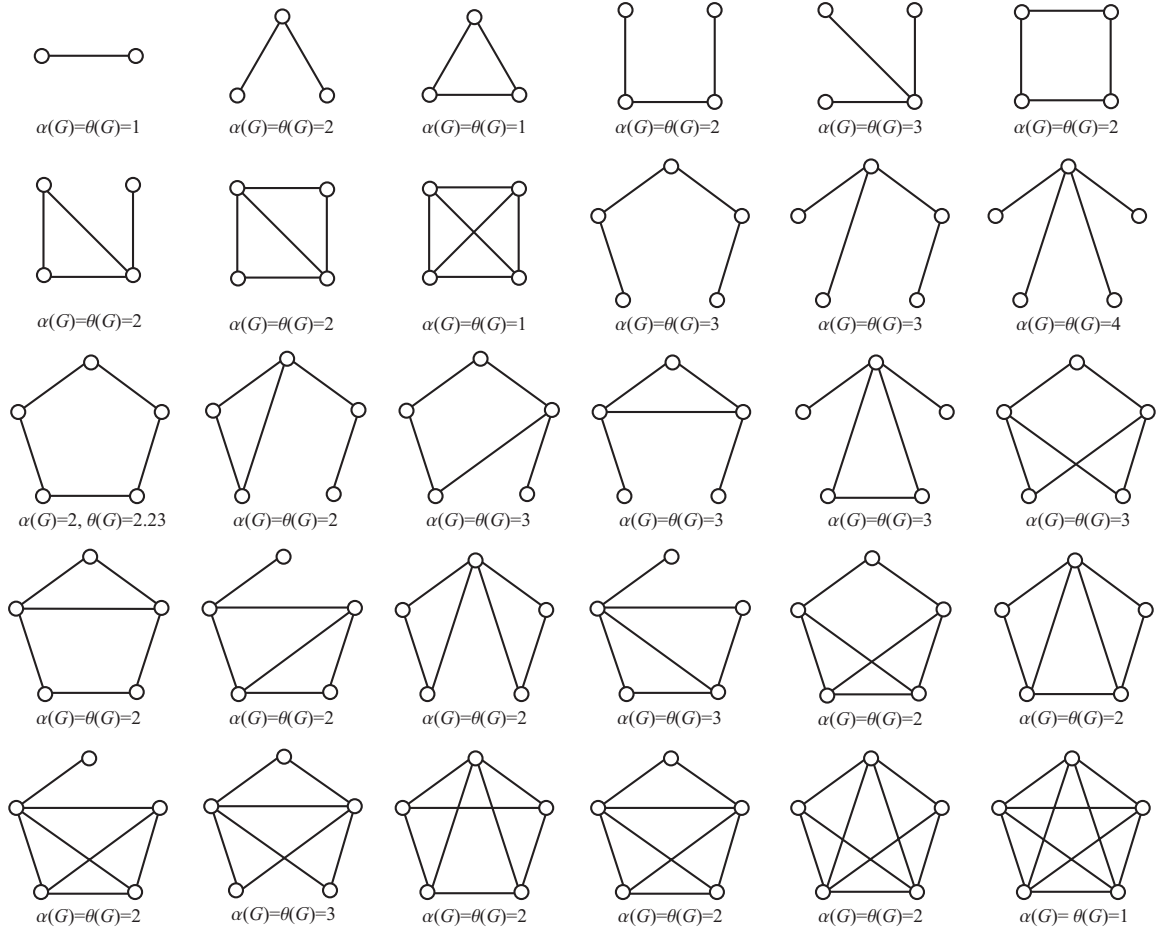
FIG. 4. Independence number $\alpha(G)$ and Lovász number $\theta(G)$ for all nonisomorphic graphs with up to 5 vertices. Only one of them, the pentagon, has $\theta(G) > \alpha(G)$.
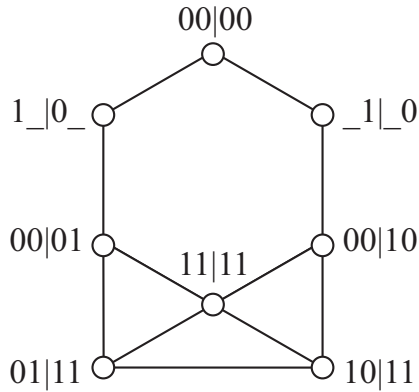

FIG. 5. Graph corresponding to the CH inequality.

C. Comparison with other Bell inequalities

The CH inequality.—The CH inequality [18] is usually

written as,

$$
P(00|00) + P(00|01) + P(00|10) \\
- P(00|11) - P(0\_|0\_) - P(\_0|\_0) \le 0. \quad (13)
$$

To obtain its graph, it must be rewritten as

$$
P(00|00) + P(00|01) + P(00|10) \\
+ P(01|11) + P(10|11) + P(11|11) \quad (14) \\
+ P(1\_|0\_) + P(\_1|\_0) \le 3.
$$

The corresponding graph is illustrated in Fig. 5.

Nonsignaling implies that $P(1\_|0\_)$ must be equal to $P(1\_|0y)$ and that $P(\_1|\_0)$ must be equal to $P(\_1|x0)$ for any choice of settings x and y. This allows one to allocate the arbitrary settings so that the probabilities in (14) combine to an inequality corresponding to a pentagon.

$$
P(11|00) + P(00|01) + P(\_1|\_1) \\
+ P(10|11) + P(00|10) \le 2. \quad (15)
$$

A different allocation of the arbitrary settings leads to an

equivalent inequality corresponding to a heptagon.

$$P(00|00) + P(1\_|0\_) + P(00|01)$$
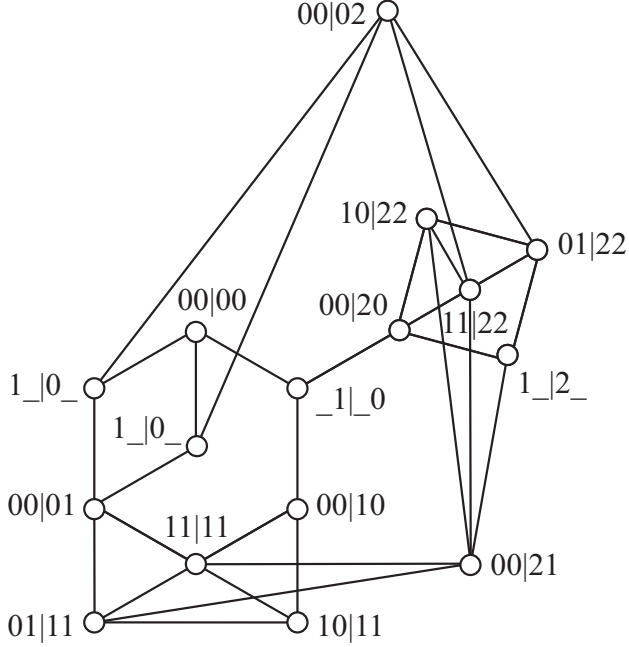$$+ P(\_1|\_1) + P(10|11) + P(00|10) \qquad (16)$$
$$+ P(\_1|\_0) \leq 3.$$

FIG. 6. Graph associated to the I_{3322} Bell inequality.

The I_{3322} Bell inequality.—The I_{3322} inequality [7–9] is a Bell inequality with three settings for Alice and Bob, each having two outputs. It reads

$$- 2P(0\_|0\_) - P(0\_|2\_) - P(\_0|\_0)$$
$$+ P(00|00) + P(00|01) + P(00|02)$$
$$+ P(00|10) - P(00|11) \qquad (17)$$
$$+ P(00|20) + P(00|21) - P(00|22) \leq 0,$$

and can be rewritten as

$$2P(1\_|0\_) + P(1\_|2\_) + P(\_1|\_0)$$
$$+ P(00|00) + P(00|01) + P(00|02)$$
$$+ P(00|10) + P(01|11) + P(10|11) + P(11|11) \qquad (18)$$
$$+ P(00|20) + P(00|21)$$
$$+ P(01|22) + P(10|22) + P(11|22) \leq 6.$$

The corresponding graph is illustrated in Fig. 6.

The I_{3322} inequality can be simplified as follows: Rewrite $P(01|11) + P(10|11) + P(11|11)$ as $P(\_1|\_1) + P(10|11)$, and $P(01|22) + P(10|22) + P(11|22)$ as $P(\_1|\_2) + P(10|22)$. Notice that $P(1\_|0\_) + P(\_1|\_0) + P(00|00) = 1 + P(11|00)$, and $P(1\_|0\_) + P(\_1|\_0) + P(00|00) = 1 + P(11|01)$. This produces the following inequality:

$$P(00|02) + P(11|01) + P(10|11) + P(00|10) + P(11|00) +$$
$$+ P(00|20) + P(10|22) + P(\_1|\_2)$$
$$+ P(00|21) + P(1\_|2\_) \leq 4.$$
$$(19)$$

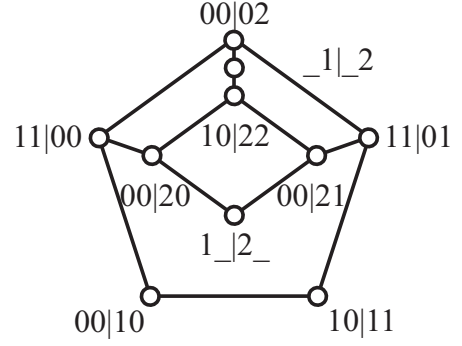The associated graph is in Fig. 7.

FIG. 7. Another graph associated to the I_{3322} Bell inequality.

D. Noncontextual inequality with the largest violation for the pentagon

In the main text, we have seen that the largest quantum violation of a bipartite Bell inequality associated to a pentagon is $\frac{3+\sqrt{2}}{2} \approx 2.207$, while the local bound is 2. However, the fact that the Lovász number of the pentagon is $\sqrt{5} \approx 2.236$ tells us that there must be a noncontextual inequality associated to a pentagon such that there is a quantum state $|\psi\rangle$ and a set of observables giving $\sqrt{5}$. For example, the noncontextual inequality can be

$$P(01|01)+P(01|12)+P(01|23)+P(01|34)+P(01|40) \leq 2,$$
$$(20)$$

where the two measurements in each probability are not local measurements but compatible measurements that can be performed in any order. A single qutrit prepared in the state [2]

$$\langle\psi| = (0, 0, 1) \qquad (21)$$

and the measurements $i = 2|v_i\rangle\langle v_i| - \mathbb{1}$ with

$$\langle v_0| = N_0 \left(1, 0, r\right), \qquad (22a)$$
$$\langle v_{1,4}| = N_1 \left(c, \pm s, r\right), \qquad (22b)$$
$$\langle v_{2,3}| = N_2 \left(C, \mp S, r\right), \qquad (22c)$$

where $r = \sqrt{\cos\left(\frac{\pi}{5}\right)}$, $c = \cos\left(\frac{4\pi}{5}\right)$, $s = \sin\left(\frac{4\pi}{5}\right)$, $C = \cos\left(\frac{2\pi}{5}\right)$, $S = \sin\left(\frac{2\pi}{5}\right)$, and N_i are suitable normalization factors, give $\sqrt{5}$ for the left hand side of (20).